Comparative study of the binary icosahedral quasicrystal $Cd_{5.7}Yb$ and its crystalline 1/1-approximant Cd_6Yb by positron annihilation spectroscopy

K. Sato and Y. Kobayashi
National Institute of Advanced Industrial Science and Technology (AIST), 1-1-1 Higashi, Tsukuba, Ibaraki 305-8565, Japan

K. Arinuma and I. Kanazawa
Department of Physics, Tokyo Gakugei University, 4-1-1 Koganei, Tokyo 184-8501, Japan

R. Tamura, T. Shibuya, and S. Takeuchi
Department of Materials Science and Technology, Tokyo University of Science, Noda, Chiba 278-8501, Japan
(Received 12 November 2003; revised manuscript received 26 April 2004; published 16 September 2004)

Previously, we showed that the icosahedral quasicrystal $Cd_{5.7}Yb$ possesses similar structural vacancies to those in its cubic 1/1-approximant Cd_6Yb by positron lifetime measurements [K. Sato, H. Uchiyama, K. Arinuma, I. Kanazawa, R. Tamura, T. Shibuya, and S. Takeuchi, Phys. Rev. B **66**, 052201 (2002)]. In the present paper, the local chemical environment around the structural vacancies is specifically investigated by two-detector coincident Doppler broadening spectroscopy. Essentially the same annihilation sites with Cd-rich chemical environments are identified for the two phases. This strongly suggests that the quasicrystal is composed of the same cluster as the approximant. The difference in the structural vacancy density between the two phases is examined by positron diffusion experiments using a slow positron beam. The structural vacancy density in the quasicrystal is found to be 20% lower than that in the approximant.

DOI: 10.1103/PhysRevB.70.094107 PACS number(s): 61.44.Br, 78.70.Bj, 41.75.Fr, 71.20.Lp

I. INTRODUCTION

Recently, a stable icosahedral quasicrystal (QC) was found in the binary Cd-Yb system.[1,2] This is not only the first stable two-component QC but also a peculiar system in view of the electronic transport[3,4] and the atomic structure.[5] The binary Cd-Yb QC is a stoichiometric compound with a very narrow single-phase region unlike existing ternary systems, suggesting the absence of chemical disorder, i.e., constitutional disorder. With this respect, Tamura *et al.*[6] have found that the temperature coefficient of the resistivity (TCR) is positive for the binary QC and it changes to negative by the addition of dilute Mg, suggesting that the negative TCR observed in ternary QC's is due to chemical disorder. There exists a cubic crystalline 1/1-approximant in the close vicinity of the composition of the QC as described by Takakura *et al.*,[5] who have shown that its structure is closely related to that of the QC. The atomic cluster of the Cd-Yb QC deduced from the structure of the approximant is completely different from that in Mackay-[7] and Bergman *et al.*[8]-type QC's. This kind of atomic cluster is composed of a Cd_4 tetrahedron inside a Cd_{20} dodecahedral shell which is surrounded by a Yb_{12} icosahedral shell.[9]

Little information has been obtained for the atomic structures of QC's due to the lack of periodicity. In this situation, a direct comparison between the QC and the approximant will be of great importance for clarifying the nature of QC's in terms of the common local structure and the different long-range orders.

As the difference between the approximants and the corresponding QC's is believed to arise only from that in the long-range order of the cluster arrangement, the structural and electronic properties of QC are often studied by making use of the approximants. Comparative studies by several experimental methods have already been performed for the binary Cd-Yb QC and its approximant. ^{170}Yb Mössbauer spectroscopy showed that the local Yb environment is quite similar for the QC and related phases.[10] Low-temperature ultra high resolution photoemission spectroscopy showed that the dip at the Fermi level is deeper for the QC than for the corresponding approximant.[11] Recently, we showed that both the QC $Cd_{5.7}Yb$ and its approximant Cd_6Yb have a single positron lifetime component with $\sim 232 \pm 3$ ps.[12] The result indicates that the quasicrystal possesses the same structural vacancies as those in the approximant. In this paper, we focus on the local chemical environment around the structural vacancies and the difference in the arrangement of the cluster between the two phases.

II. EXPERIMENT

Alloys of the icosahedral QC and the cubic 1/1-approximant with nominal compositions $Cd_{84.6}Yb_{15.4}$ and $Cd_{85.7}Yb_{14.3}$, respectively, were prepared by the procedure, which is detailed elsewhere.[12] The obtained alloys $Cd_{84.6}Yb_{15.4}$ and $Cd_{85.7}Yb_{14.3}$ were a single quasicrystalline and 1/1-approximant phase, respectively, as confirmed by powder x-ray diffraction spectroscopy with Cu $K\alpha$ radiation having an angle resolution of 0.06 Å. Each alloy ingot was cut into a 2 mm thick disc with 9 mm in diameter for the present experiments.

For the lifetime measurements, the positron source (^{22}Na), sealed in a thin foil of Kapton, was mounted in a sample-source-sample sandwich. The positron annihilation lifetime spectra ($\sim 1 \times 10^6$ coincidence counts) with a time resolution of 280 ps full width at half maximum (FWHM) were re-

corded at room temperature. After subtracting the background, the data were numerically analyzed using the POSITRONFIT code.[13]

The coincident measurements were performed by measuring the energies of the two annihilation quanta E_1 and E_2 with a collinear setup of two high-purity Ge detectors with 1.0 keV (FWHM) energy resolution. The Doppler broadening spectra were obtained by cutting the E_1, E_2 spectra along the energy conservation line $E_1+E_2=(1022\pm1)$ keV, taking into account the annihilation events within a strip of ±1.6 keV. Details on coincident Doppler broadening spectroscopy are given elsewhere.[14]

Positron diffusion behavior in the two phases was investigated by Doppler broadening measurements with a magnetically guided positron beam coupled with a high purity Ge detector. The energy resolution of the detector was ~1 keV (FWHM). More information about the apparatus used in the present experiments can be found in Ref. 15. Doppler broadening spectra were analyzed by taking the *S* parameter, which was determined by the ratio of the central area over (−0.7-+0.7) keV to the total area of the Doppler broadening spectra after subtracting the background. The measurement was repeated nine times in order to obtain good statistical precision.

III. RESULTS AND DISCUSSION

The lifetime measurements for the present samples showed a single component with lifetimes τ_1 of 240±4 ps and 237±4 ps for QC $Cd_{84.6}Yb_{15.4}$ and approximant Cd_6Yb, respectively, in good agreement with the previous measurements.[12] In order to examine the local chemical environment around the annihilation sites, coincident Doppler broadening measurements were performed for the two phases. Figure 1 shows the high-momentum Doppler broadening spectra of the QC and approximant together with those of pure metals. Figure 1(a) shows the raw spectra whereas the ratio representation normalized to the pure Cd spectrum are shown in Fig. 1(b).

The Doppler spectra of the QC and approximant are slightly different from each other in the momentum region around 5×10^{-3} m_0c. This may reflect the different electronic structure in the valence electron region between the two phases. In the core electron region higher than 20×10^{-3} m_0c, the spectra are essentially identical to each other, indicating the same chemical surroundings of the trapping sites [see Fig. 1(a)]. By comparing the raw spectra with the pure Cd spectrum in the inset of Fig. 1(a), we find that the chemical surroundings of the trapping site are dominated by Cd atoms. The ratio spectra in Fig. 1(b) clearly exemplify Cd-rich chemical surroundings of the vacancies in the QC and approximant.

For the approximant, the first shell inside the Cd_{20} dodecahedral second shell consists of four Cd atoms, which occupy four sites among equivalent eight sites, the other four sites remaining vacant.[9] Four Cd atoms placed at vertices of a small cube with an occupancy of 0.5 form a tetrahedron. The Cd vacant sites with Cd-rich surroundings in the approximant are the trapping sites of positrons.

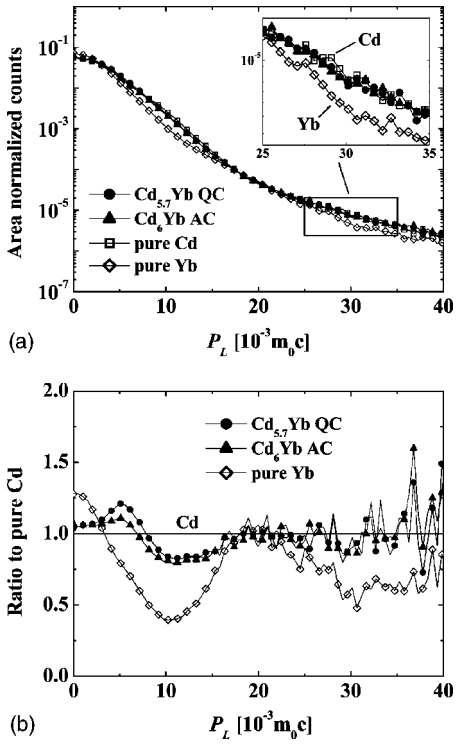

FIG. 1. (a) Coincident Doppler broadening spectra of the icosahedral QC $Cd_{5.7}Yb$ (full circles) and cubic crystalline 1/1-approximant Cd_6Yb (full triangles) together with those of pure Cd (open squares) and pure Yb (open diamonds). Each spectrum is normalized by the total number of counts. The inset shows the blown-up section in the high-momentum core electron region. (b) Doppler broadening ratio spectra taken from Fig. 1(a). Each spectrum is normalized to the Doppler broadening spectrum of pure Cd (horizontal line).

Judging from essentially the same positron lifetime and Cd-rich chemical environment observed in the QC, the following picture can be reasonably presented. The QC is composed of the same local cluster units as that in the approximant, where the tetrahedron with four Cd atoms is located at the center. Positrons are localized after thermalization around the 4 Cd tetrahedra inside the dodecahedral shell of 20 Cd in the two phases and are annihilated therein.

Since we found the same local structure between the QC and the approximant, the question is now how differently clusters are ordered in the two phases, i.e., the difference in the density of the trapping sites. To answer this question, positron diffusion experiments using a slow positron beam were performed. Figure 2 shows the *S* parameter for the QC (open squares) and approximant (full squares) as a function of positron incident energy and mean implantation depth (*S*-*E* plot). It is clearly seen from Fig. 2 that the measured *S* parameters for the two phases increase in the energy region from 0 to 10 keV, beyond which they are saturated. The rapid increase, typical for the QC's and their related materials, is due to the dense distribution of structural vacancy-type sites giving rise to the saturation positron trapping.[12]

We note that the *S* parameter for the QC increases more slowly than the approximant in the shallow energy range from 0 to 10 keV (see inset in Fig. 2). The similar surface *S*

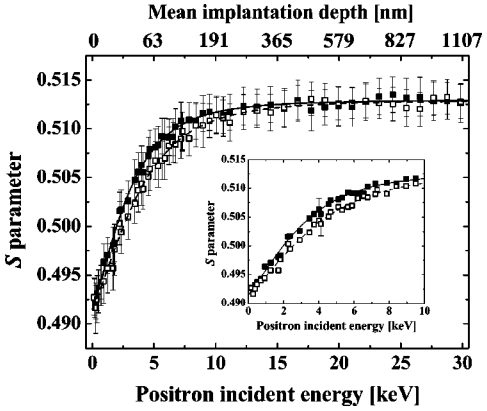

FIG. 2. Measured S parameter data for the icosahedral QC $Cd_{5.7}Yb$ (full squares) and cubic crystalline 1/1-approximant Cd_6Yb (open squares) as a function of positron incident energy. In addition to the energy abscissa scale, implantation depth scale according to the Eq. (3) is given. The solid and dashed lines are results of the weighted nonlinear square fit for the cubic crystalline 1/1-approximant Cd_6Yb and icosahedral QC $Cd_{5.7}Yb$, respectively. The inset shows the blown-up section in the energy range from 0 to 10 keV.

parameters at the lowest incident energy for the two samples indicate that no surface effect is involved in the dissimilar variations of the S parameters with incident energy. Hence, the data in Fig. 2 demonstrates the lower positron diffusivity in the bulk of the approximant than that of the QC. The distinct positron diffusivities arise from the difference of the density of trapping sites between the two phases.

According to the x-ray structural analysis by Larson and Gromer,[16] the Cd_4 tetrahedron in the approximant would be disposed in one of six possible orientations. Furthermore, Tamura *et al.*[20] observed that the Cd_4 tetrahedra are orientationally ordered at low temperatures, i.e., the central Cd_4 tetrahedra is ordered below 110 K. From the estimated low activation energy, they suggested high frequency rotation of the Cd_4 tetrahedra at room temperature. On the basis of these reports, we expect that the Cd_4 tetrahedra are in highly disordered state in the approximant.

We have applied the scaling method[17–19] to the structure with four Cd atoms placed inside the dodecahedral second shell. The average positron-diffusion length L_+ can be generally estimated from the analysis of the S-E plot. After implantation with E, positrons rapidly lose energy (E) and reach thermal equibrium with the medium within a few pico seconds. The spatial distribution of the thermalized positrons $\tilde{P}(E,z)$ along the incident direction (z) can be described by a scaling function[17,18]

$$\tilde{P}(E,z) = N_{lm}\left(\frac{u}{C_{lm}}\right)^{l}\exp\left[-\left(\frac{u}{C_{lm}}\right)^{m}\right], \tag{1}$$

where N_{lm} is a normalization constant, and C_{lm}, l, and m are parameters which depend on material in consideration,[18,19] and u is defined as

$$u = \frac{z}{\langle z(E)\rangle}, \tag{2}$$

where $\langle z(E)\rangle$ is the mean implantation depth. $\langle z(E)\rangle$ is assumed to be given by

$$\langle z(E)\rangle = \frac{A_i}{\rho_i}E^{\alpha_i+\beta_i lnE}, \tag{3}$$

where E and ρ_i are the incident energy of the positron beam and the density of the sample, respectively. The parameters A_i, α_i, and β_i depend on the atomic number of the constituent elements as confirmed by Monte Carlo simulation.[21]

After thermalization, positrons begin to diffuse in the sample. The one-dimensional positron diffusion is described by the following equation:

$$D_+\frac{\partial^2 N(z,t)}{\partial z^2} - \frac{\partial N(z,t)}{\partial t} - \Gamma N(z,t) = 0, \tag{4}$$

where D_+ is the positron diffusion coefficient, $N(z,t)$ is the positron density as a function of both time and position, and Γ is the effective annihilation rate of the positron. The observed S parameter is given by a linear combination ofcontributions from different annihilation sites

$$S(E) = \sum_i S_i F_i(E), \tag{5}$$

where $F_i(E)$ is the fraction of positrons annihilating in the i-th state characterized by the S_i parameter. The fraction $F_i(E)$ can be obtained by solving the diffusion equation, subjected to the positron implantation profile and boundary conditions. By fitting the measured S parameters to Eq. (5), one can obtain the average positron-diffusion length L_+.

During the positron diffusion from bulk to surface, thermalized positrons are localized around the tetrahedron inside the dodecahedral shell if they are within a certain radius r_t (average positron-trapping radius) from the center of the tetrahedron. Since only a single component is observed in the positron lifetime of the approximant,[12] Eq. (5) can be rewritten as

$$S = S_s F_s + S_b F_b, \tag{6}$$

where S_s and S_b are the S parameters, and F_s and $F_b(=1-F_s)$ are the annihilation rates for surface and bulk states, respectively. We assume that the density of the trapping sites in the approximant is given by $2/a^3$, where a is the lattice constant ($a=15.64$ Å). By calculating the probability of the thermalized positron diffusing without trapped around the tetrahedron, we obtain the average positron-diffusion length in the approximant as a function of the trapping radius r_t. A solid line in Fig. 2 gives the result of a fit performed by the weighted nonlinear least-squares method, and the trapping radius r_t is determined to be ~3 Å for the approximant.

Since the QC and the approximant have a similar local atomic structure as suggested from the positron lifetime and high momentum Doppler broadening spectroscopy, we assume the same trapping radius of ~ Å in obtaining the density of the trapping sites in the QC. The result of the weighted nonlinear least-squares fit is shown in Fig. 2. The

TABLE I. Structural vacancy density C in the icosahedral QC $Cd_{5.7}Yb$ together with that of the cubic crystalline 1/1-approximant Cd_6Yb. The values of the average positron-diffusion length L_+ are given as well.

Specimen	C [10^{20} cm^{-3}]	L_+ [Å]
QC $Cd_{5.7}Yb$	4.1	556
Cubic Cd_6Yb	5.2	399

density of the trapping sites for the QC is obtained as 4.1×10^{20} cm^{-3} Here, it should be mentioned that in our model the trapping site density is equivalent to the structural vacancy density. Table I lists the structural vacancy density C in the QC and approximant. It can be seen that the structural vacancy density in the QC is lower by 20% than in the approximant.

The statistical error in the trapping site density obtained by the data analysis mentioned above is discussed here. The fluctuations of the average positron-diffusion length (δL_+) and the trapping radius (δr_t) in the approximant are $\sim$43 Å and $\sim$0.1 Å, respectively, as estimated from the measured S-E plot. The fluctuation of the trapping site density (δC) for the QC is estimated to be 0.21×10^{20} cm^{-3} according to the law of error propagation in the rest of the calculation process. Note that the error of 0.21×10^{20} cm^{-3}($\sim$5%) is small enough to compare the structural vacancy density between the two phases. The difference of 20% derived from the present data analysis is therefore reliable.

IV. CONCLUSIONS

In the previous paper, we predicted that the icosahedral quasicrystal $Cd_{5.7}Yb$ possesses similar structural vacancies to those in its cubic 1/1-approximant Cd_6Yb by positron lifetime measurements.[12] In the present paper, the local chemical environment around the structural vacancies was specifically investigated by two-detector coincident Doppler broadening spectroscopy. Essentially the same type of annihilation sites with Cd-rich chemical environment were identified for the two phases. This strongly suggests that the icosahedral QC $Cd_{5.7}Yb$ is composed of the same cluster as the cubic crystalline 1/1-approximant Cd_6Yb. The difference in the structural vacancy density between the two phases was clearly detected by the slow positron beam experiments. The structural vacancy density in the icosahedral QC $Cd_{5.7}Yb$ was deduced to be 4.1×10^{20} cm^{-3}, which is 20% lower than that of the approximant. This lower density should be taken into account for the structure modeling of the Cd-Yb QC. The quantitative information as demonstrated in this work is of importance for future studies of the atomic structure of the icosahedral QC $Cd_{5.7}Yb$.

ACKNOWLEDGMENT

This work was supported by the New Energy and Industrial Technology Development Organization (NEDO).

[1] A. P. Tsai, J. Q. Guo, E. Abe, H. Takakura, and T. J. Sato, Nature (London) **408**, 537 (2000).
[2] J. Q. Guo, E. Abe, and A. P. Tsai, Phys. Rev. B **62**, R14 605 (2000).
[3] R. Tamura, Y. Maruo, S. Takeuchi, K. Tokiwa, T. Watanabe, T. J. Sato, and A. P. Tsai, Jpn. J. Appl. Phys., Part 2 **40**, L912 (2001).
[4] Y. Ishii and T. Fujiwara, Phys. Rev. Lett. **87**, 206408 (2001).
[5] H. Takakura, J. Q. Guo, and A. P. Tsai, Philos. Mag. Lett. **81**, 411 (2001).
[6] R. Tamura, T. Araki, and S. Takeuchi, Phys. Rev. Lett. **90**, 226401 (2003).
[7] A. L. Mackay, Acta Crystallogr. **15**, 916 (1962).
[8] G. Bergman, J. L. T. Waugh, and L. Pauling, Acta Crystallogr. **10**, 254 (1957).
[9] A. Palenzona, J. Less-Common Met. **25**, 367 (1971).
[10] D. H. Ryan, N. M. Saleema, R. Gagnon, and J. van Lierop, J. Phys.: Condens. Matter **13**, 10159 (2001).
[11] R. Tamura, Y. Murao, S. Takeuchi, T. Kiss, T. Yokoya, and S. Shin, Phys. Rev. B **65**, 224207 (2002).
[12] K. Sato, H. Uchiyama, K. Arinuma, I. Kanazawa, R. Tamura, T. Shibuya, and S. Takeuchi, Phys. Rev. B **66**, 052201 (2002).
[13] P. Kirkegaard and M. Eldrup, Comput. Phys. Commun. **7**, 401 (1974).
[14] P. Asoka-Kumar, M. Alatalo, V. J. Ghosh, A. C. Kruseman, B. Nielsen, and K. G. Lynn, Phys. Rev. Lett. **77**, 2097 (1996).
[15] Y. Kobayashi, I. Kojima, S. Hishita, T. Suzuki, E. Asari, and M. Kitajima, Phys. Rev. B **52**, 823 (1995).
[16] A. C. Larson and D. T. Cromer, Acta Crystallogr., Sect. B: Struct. Crystallogr. Cryst. Chem. **27**, 1875 (1970).
[17] V. J. Ghosh, D. O. Welch, and K. G. Lynn, in *Proceeding 5th International Workshop on Slow Positron Beams for Solids and Surface*, edited by E. H. Ottewitte (AIP, New York, 1992), p. 937.
[18] V. J. Ghosh, Appl. Surf. Sci. **85**, 187 (1995).
[19] G. C. Aers, P. A. Marshall, T. C. Leung, and R. D. Goldberg, Appl. Surf. Sci. **85**, 196 (1995).
[20] R. Tamura, Y. Maruo, S. Takeuchi, M. Ichihara, M. Isobe, and Y. Ueda, Jpn. J. Appl. Phys., Part 2 **41**, L524 (2002).
[21] G. C. Aers, J. Appl. Phys. **76**, 1622 (1994).